The D(p, d^*)p Cross Section from the D(p, $2p$)n Reaction*

A. NIILER†
Los Alamos Scientific Laboratory, University of California, Los Alamos, New Mexico 87544
AND
W. VON WITSCH‡ AND G. C. PHILLIPS
Rice University, Houston, Texas 77001
AND
C. JOSEPH†
University of Lausanne, Lausanne, Switzerland
AND
V. VALKOVIĆ†
Institut Ruđer Bošković, Zagreb, Yugoslavia

(Received 16 June 1969)

Three-body breakup spectra from a kinematically complete measurement of the D(p, $2p$)n reaction have been analyzed to yield the cross section for the production of d^*, a quasiparticle consisting of a neutron and proton in a $^1S_0$ configuration. An excitation function of the D(p, d^*)p reaction is obtained for the proton bombarding energy range 9–13 MeV. In agreement with measurements and predictions of the (p, d^*) cross section on several nuclei, the D(p, d^*)p cross section is about an order of magnitude less than the elastic D(p, d)p cross section. The D(p, d^*)p excitation function shows a peak at the bombarding energy $E_p=10.25$ MeV which coincides with a ^{3}He excitation energy of 12.4 MeV. This peak might be interpreted as either a state in ^{3}He or a threshold effect.

INTRODUCTION

A NUMBER of recently studied reactions involving three particles in the final state, two of which are a neutron and proton, have exhibited a strong final-state interaction (FSI) between the neutron and a proton in a $^1S_0$ configuration. Although this FSI has been observed in kinematically incomplete experiments,[1] the most clearly defined evidence comes from kinematically complete experiments.[2] In general, the three-body final state is produced via a two-step sequential decay mechanism described by the equation

$$b+T\rightarrow(np)+X\rightarrow n+p+X, \qquad (1)$$

where b and T are the bombarding and target particles, respectively. In an incomplete experiment, only one of the three final-state particles is detected, while in a complete experiment, usually the proton along with the neutron *or* particle X have their momenta measured in coincidence. The fact that the reaction described in Eq. (1) involves sequential decay implies that in the first step, the neutron and proton must behave as a single particle long enough to allow X to escape their radius of interaction and then the system proceeds to the second step in which the quasiparticle decays into a neutron and proton.

This n-p quasiparticle has been referred to as the virtual singlet state of the deuteron. However, the singlet state of the deuteron is described by an S-matrix pole on the negative imaginary axis in the complete k plane and, thus, it is a virtual, physically unobservable state. On the other hand, Phillips, Griffy, and Biedenharn[3] (PGB) have modified Wigner's[4] formulation to show that for a system of two particles within a radius a, each partial wave will have a time delay in decaying given approximately by

$$\Delta T_l=\hbar(d/dE)[\delta_l+\phi_l(a)]. \qquad (2)$$

δ_l is the lth partial wave phase shift, ϕ_l is the hard-sphere phase shift, and E is the relative energy between the particles. Now, since this S-matrix pole corresponding to the virtual singlet state of the deuteron lies relatively close to the real k axis, it influences the n-p singlet phase shift in such a way that the ΔT of Eq. (2) begins at a maximum value at $E=0$ and decreases monotonically with increasing energy.

This time delay at a relative energy of 60 keV is approximately 3×10^{-22} sec during which time the first emitted proton travels about 72 fm. Thus, at the time that the interacting particles "break up," the first emitted proton is well outside the range of their interaction. This time delay in the decay of the n-p system at

* Work performed under the auspices of the U.S. Atomic Energy Commission.
† A large part of the work was accomplished while these authors were at Rice University.
‡ On leave from Max-Planck-Institut für Kernphysik, Heidelberg, Germany.
[1] M. Cerineo, K. Ilakovac, I. Slaus, P. Tomaš, and V. Valković, Phys. Rev. **133**, B948 (1964); A. S. Clough, C. J. Batty, B. E. Bonner, C. Tschalar, and L. E. Williams, Nucl. Phys. **A121**, 689 (1968).
[2] W. D. Simpson, W. R. Jackson, and G. C. Phillips, Nucl. Phys. **A103**, 97 (1967); H. Brückmann, W. Klüge, and L. Schanzler, Z. Physik **217**, 350 (1968).
[3] G. C. Phillips, T. A. Griffy, and L. C. Biedenharn, Nucl. Phys. **21**, 327 (1960).
[4] E. P. Wigner, Phys. Rev. **98**, 145 (1955).

relative energies near zero gives rise to a broad peak in the "three-body" yield. Thus, one can speak of an entity composed of a neutron and proton in a $^1S_0$ configuration which behaves similar to a short-lived particle. Henceforth, this quasiparticle is labeled d^*.

It is possible to produce d^* in the reaction of Eq. (1) only if the kinematic conditions are such that low n-p relative energies are allowed. The nonrelativistic three-body kinematics have been calculated in full in Ref. 5.

In the case of a reaction

$$b+T\rightarrow A+X\rightarrow a+c+X, \qquad (3)$$

under certain conditions, information about the composite state A can be obtained by the detection of any one of the final-state particles a, c, or X. No matter which particle is detected, a and c must be different from X in order to eliminate the indeterminacy created by the lack of knowledge of the order of the emission of identical particles. The breakup particles a and c will be confined to a cone whose half angle is given by $\sin\theta_{1/2}=v_{\rm int}/v_A$, where $v_{\rm int}$ is half the relative velocity of a or c in A and v_A is the velocity of particle A. Thus, if either a or c is to be detected, $v_{\rm int}$ must be small enough or v_A large enough so that $\theta_{1/2}$ is not larger than the half angle of the detector $\phi_{1/2}$. Otherwise, any peaks may be averaged out by contributions from the A's which are emitted at angles adjacent to the observed angle. The condition $\theta_{1/2}\leq\phi_{1/2}$ is very difficult to meet for many experiments with good geometry. As an example, for the 94-keV ^{8}Be ground state, $\theta_{1/2}=5.5°$ at $E^8_{\rm Be}=10$ MeV. Consequently, an experiment involving a reaction represented by Eq. (3) from which information is to be obtained about A, which involves detecting one of the decay products of A only, is always difficult and in most cases impossible.

The situation is somewhat better if particle X is detected and, in fact, this method has been one of the more powerful spectroscopic tools. However, in cases where the state A is several MeV or more wide, or where the cross section for the reaction is very small so that most of the yield is due to various background reactions, even the detection of X might not be sufficient to obtain information about A. A large number of experiments have been performed in which A represents a nucleon-nucleon final-state interaction and X is the detected particle. A complete survey and discussion of these $T(b, X)2N$ experiments is given by van Oers and Slaus.[6] No information about the d^* has been obtained through these experiments.

Another method of obtaining information about the state A in Eq. (3) is to do a coincidence measurement of the momenta of any of the three pairs of final-state particles. Knowing the kinematics completely, as is the case when two out of the three momenta are known, is extremely useful in choosing the optimum kinematic regions for the desired measurements. This point is discussed in Ref. 7. Cohen *et al.*[8] have obtained angular distributions of the one-neutron pickup reaction (p, d^*) on several nuclei by making coincident measurements of proton and neutron energies at the same angle. Brown *et al.*[9] have measured the one-alpha pickup reaction ^{16}O(α, ^{8}Be$_{\rm gs}$)^{12}C leaving the ^{12}C in its ground and 4.44-MeV states by detecting in coincidence the breakup alphas from the ^{8}Be ground state. In both cases, the essentially geometrical corrections necessary due to the wide $\theta_{1/2}$ were straightforward because the d^* and ^{8}Be$_{\rm g.s.}$ are both in an S configuration.

The D(p, d^*)p reaction is most conveniently observed by measuring, in coincidence, the momenta of the two protons. This method allows one to distinguish between the first and second emitted protons and between the D(p, 2p) protons and those from various background producing reactions (i.e., energy-degraded elastic protons). A correction for decay protons which are deposited outside the detector solid angle is necessary but is essentially a transformation of solid angles.

One of the more interesting results obtainable from (p, d^*) reactions is information about particle-cluster states consisting of a d^* and particle X. Whereas a cluster consisting of a regular ground-state deuteron and X is capable of forming states of isospin T, where T is the isospin of X, the (d^*-X) cluster can form states of isospin $1\pm T$. Consequently, the D(p, d^*)p reaction might form either $T=\frac{1}{2}$ or $\frac{3}{2}$ states of ^{3}He. The $T=\frac{3}{2}$ possibility arises only if such a state has some admixture of $T=\frac{1}{2}$.

EXPERIMENTAL METHOD

This experiment was performed at the tandem Van de Graaff facility of the T. W. Bonner Nuclear Laboratory at Rice University. As the detailed description of the experimental procedure has been given in Ref. 7, only a short outline is discussed here. Preliminary results on the D(p, d^*)p reaction were reported in Ref. 10.

A beam of protons was used to bombard a 1-mg/cm^2-thick deuterated polyethylene foil to produce the $p+D\rightarrow p+d^*\rightarrow p+p+n$ reaction. For future reference, the first emitted proton is labeled as particle 2 or proton 2, the decay proton as particle 1 or proton 1, and the neutron as particle 3. Two silicon surface-barrier

[5] J. D. Bronson, W. D. Simpson, W. R. Jackson, and G. C. Phillips, Nucl. Phys. **68**, 241 (1965).

[6] W. T. H. van Oers and I. Slaus, Phys. Rev. **160**, 853 (1967).

[7] A. Niiler, C. Joseph, and G. C. Phillips, Bull. Am. Phys. Soc. **13**, 568 (1968); A. Niiler, C. Joseph, V. Valković, W. von Witsch, and G. C. Phillips, Phys. Rev. **182**, 1083 (1969).

[8] B. L. Cohen, E. C. May, and T. M. O'Keefe, Phys. Rev. Letters **18**, 962 (1967); B. L. Cohen, E. C. May, T. M. O'Keefe, and C. L. Fink, Phys. Rev. **179**, 962 (1969).

[9] R. E. Brown, J. S. Blair, D. Bodansky, N. Cue, and C. D. Kavaloski, Phys. Rev. **138**, B1394 (1965).

[10] A. Niiler, W. von Witsch, and G. C. Phillips, Bull. Am. Phys. Soc. **13**, 1652 (1968).

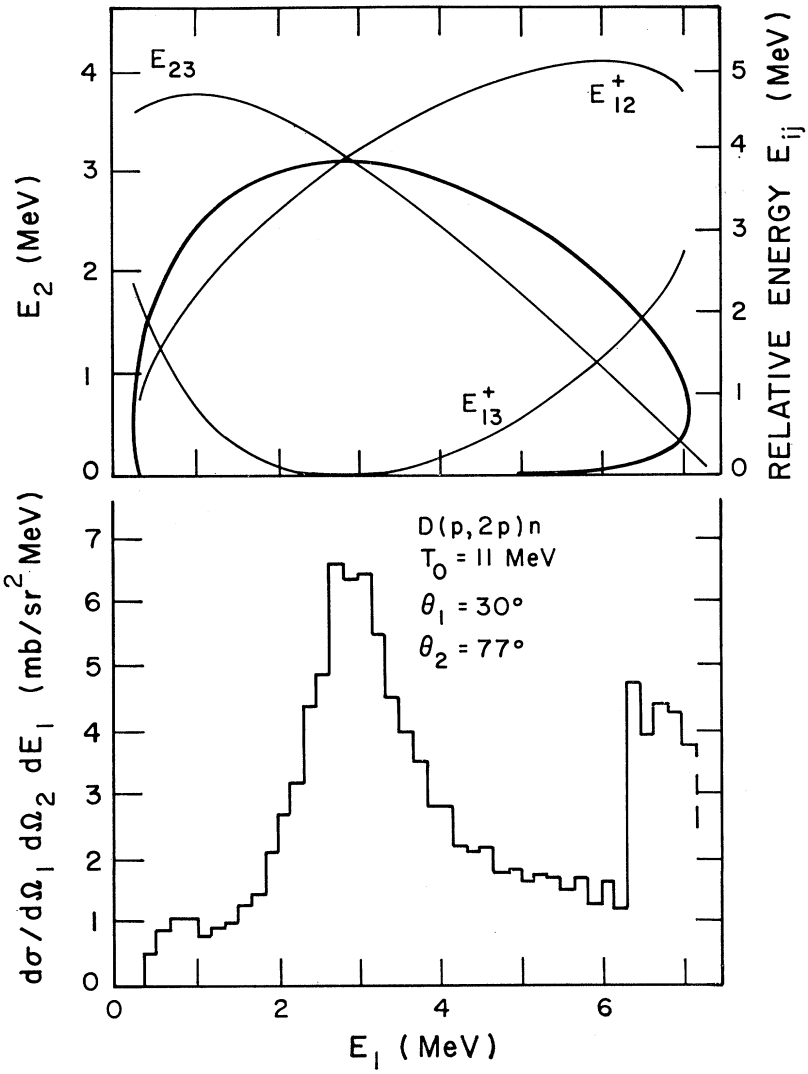

FIG. 1. Sample of the three-body kinematics and data. The heavy curved line at the top represents the kinematic locus along which events from the $D(p, 2p)n$ reaction populate the E_1-E_2 plane. The light lines give the particle-pair relative energies as a function of E_1 for the upper part of the kinematic locus. The subscript numbers are defined in the text. At the bottom, the data along the locus in the E_1-E_2 plane is shown projected on the E_1 axis. The peak at $E_1=3$ MeV is due to a final-state interaction between a proton and neutron in a $^1S_0$ state at very low energy.

detectors were used to measure, in coincidence, the energies of the two final-state protons. One detector was kept at a constant $\theta_1=30°$ angle and the other one, at angle θ_2, was moved to correspond to the first emitted proton angle when a d^* with low n-p relative energy (E_r) recoils at 30°. The two detectors were always kept on opposite sides of the beam. This choice of angles corresponded to the proton 2 and the d^* at low E_r being emitted at 180° in the p-d^* c.m. system. By doing angular correlation measurements at two energies (9 and 10.5 MeV), Simpson *et al.*[2] observed the highest laboratory yield at this set of angles, the recoil axis of the p-d^* system.

The two-dimensional energy events were stored in an IBM-180 on-line computer. To facilate background subtraction, the time-of-flight differences between the two protons were also recorded. The experiment was monitored by counting elastically recoiling deuterons in the 30° detector. Wilson's[11] p-d elastic scattering data were then used to obtain absolute cross-section values.

The coincident E_1, E_2 events are constrained to lie along a curved locus in the E_1-E_2 plane. An example of this situation is shown in Fig. 1 for $E_p=11$ MeV, $\theta_1=30°$, and $\theta_2=77°$. The heavy line in the upper part of Fig. 1 represents the E_1 versus E_2 kinematic locus while the light lines show the relative energies of different pairs of nucleons as functions of the energy in detector 1. The relative energies for only the upper part of the locus are shown since the data for the lower part is cut off by a threshold on E_2. The lower part of the figure shows the cross section for the $(p, 2p)$ reaction projected on the E_1 axis. Note that the main peak in the projected spectrum corresponds to low values of E_{13}^+, the relative energy

[11] A. S. Wilson, M. C. Taylor, J. C. Legg, and G. C. Phillips, Nucl. Phys. **A130**, 624 (1969).

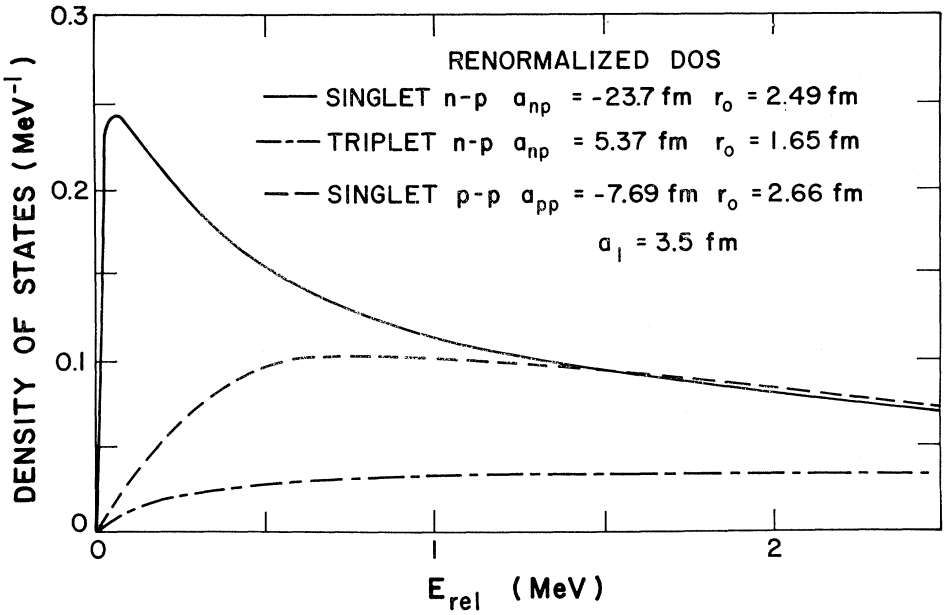

FIG. 2. PGB renormalized density of states. Shown are the singlet and triplet n-p and the singlet p-p density of states with the effective range parameters as listed. a_1 is the renormalization radius.

between the neutron and proton 1. Another peak due to the phase-space effect and $E_{23}\sim 0$ is seen around $E_1=6.5$ MeV. The small peak below 1 MeV is due to p-^{12}C elastic coincidences. The general features, except for the p-^{12}C effect, are present at all energies at which data were collected. Table I lists these energies and corresponding angles.

ANALYSIS

A particular E_1-E_2 spectrum in the D$(p, 2p)n$ reaction has contributions from a number of different final-state interactions and direct processes. However, in order to obtain the (p, d^*) differential cross section, it is necessary to isolate the contribution from that FSI in which the neutron and proton in a d^* particle are emitted in the direction of detector 1 from the contributions of the other processes. One must have a reasonably good theoretical description of the spectral structure due to all of the processes involved to estimate their relative strengths. In Ref. 7, it was shown that the PGB density-of-states formalism is quite adequate to describe the final-state interactions since a reasonably good value for the n-p singlet scattering length was obtained with it.

TABLE I. Energies and angles of the experimental data.

E_p (MeV)	θ_1	θ_2
9.00	30.0°	73.2°
9.50	30.0°	74.3°
10.00	30.0°	75.4°
10.50	30.0°	76.2°
10.75	30.0°	76.6°
11.00	30.0°	77.0°
11.25	30.0°	77.4°
11.50	30.0°	77.7°
12.00	30.0°	78.7°
12.50	30.0°	79.2°
13.00	30.0°	79.7°

The various contributing processes will now be enumerated and discussed. Figure 2 shows the n-p and p-p final-state PGB renormalized density-of-states functions. Figure 3 shows the individual structures contributing to the D$(p, 2p)n$ reaction as functions of E_1. The FSI components are calculated from the expressions given in Ref. 7 and drawn to the same arbitrary scale but the direct processes are drawn simply to exhibit their shapes.

(*1*) *Final-state interactions.* There are five possible ways in which final-state interactions can occur in the D$(p, 2p)n$ reaction. Numbering the final-state particles as in the previous section, it is possible to have the $^1S_0$ interaction in the n-p systems 1, 3 and 2, 3 and in the p-p system 1, 2. Also, the $^3S_0$ interaction is possible in the 1, 3 and 2, 3 neutron-proton systems. In Fig. 2 the PGB generalized density of states are plotted as functions of the particle-pair relative energies for the n-p singlet and triplet and the p-p singlet cases. The effective range parameters used are shown. a_1 is the radius of renormalization of the wave functions. A particle-pair c.m.-to-laboratory solid-angle transformation along the kinematic locus shown in Fig. 1 along with projection onto the E_1 axis is required to obtain the FSI curves in Fig. 3 from the density-of-states curves in Fig. 2.

(*2*) *Quasifree process.* Although the quasifree process

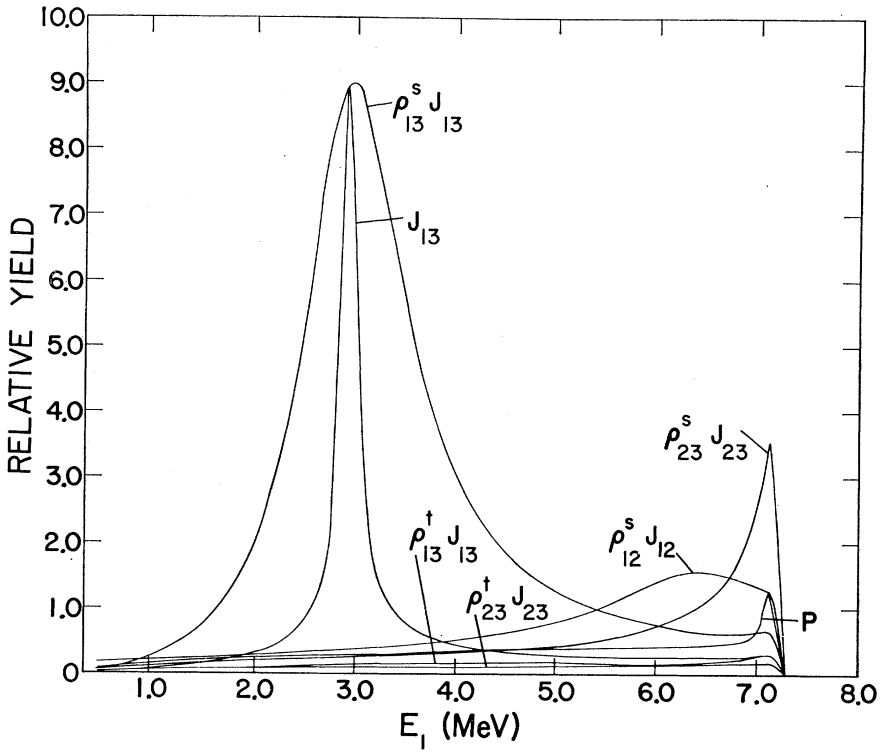

FIG. 3. Processes contributing to the $D(p, 2p)n$ reaction at $E_p=$ 11 MeV. The final-state interaction terms, indicated by $\rho_{ij}{}^{s,t}J_{ij}$, are the density-of-states functions of Fig. 2 transformed from the ij c.m. system to the lab. The FSI terms are calculated exactly but drawn to the same arbitrary scale. The phase space designated by P and the solid-angle transformation term designated by J_{13} are also shown.

can be quite strong in a kinematic region where the spectator (i.e., the undetected neutron in this case) energy is very low, its contribution is negligible in regions where the E_n remains above 1 MeV. This latter condition is met for all spectra in this set of data (see Ref. 7) so this process is neglected.

(3) *Kinematic effects.*

(a) Phase space: When the initial state transforms into a final state in which the three particles are emitted simultaneously, the energy states of the final-state particles are populated according to the phase space available to them. This phase space is given by

$$P_T=\int_{i=1,3}^{P_i,\Omega_i}\prod_i P_i^2 dP_i d\Omega_i \delta[E_0-\sum_i (P_j^2/m_j)] \times\delta(\bar{P}_0-\sum_k \bar{P}_k),$$

where the δ functions conserve energy and momentum. Upon integration over the δ functions and transformation from momentum to energy space, the phase space becomes

$$P_T=\int_{E_1}\int_{\Omega_1}\int_{\Omega_2} P(E_1, \Omega_1, \Omega_2)\, dE_1 d\Omega_1 d\Omega_2,$$

where

$$P(E_1, \Omega_1, \Omega_2) = \frac{m_1 m_3 P_1 P_2^2}{|P_2[(m_2+m_3)/m_2]+P_1\cos\theta_{12}-P_0\cos\theta_2|}.$$

P_1 and P_2 are the momenta of the protons observed in detectors 1 and 2, respectively, and $\theta_{12}=\theta_1+\theta_2$. The shape of this phase space is smooth over a large part of E_1 and has a sharp peak near the maximum in E_1. Simpson *et al.*[2] have displayed the phase space for a number of energy-angle combinations.

(b) Solid-angle transformation: In order to get a peak in the coincidence yield at a low relative energy of one of the particle pairs, it is not necessary for the density-of-states (DOS) function to have any particular form. Even if the DOS function were constant for all relative energies (which, of course, it is not), one would see a peak in the laboratory yield in regions where E_r is so low that $\theta_{1/2}<\phi_{1/2}$ (see the Introduction). This effect is due solely to the Jacobian which transforms the detector solid angles from the recoil c.m. system (the system in which a given interacting particle pair is at rest) to the overall c.m. system. This illustrates the fact that it is not necessarily the appearance of a peak at low E_r which gives information about a particular final-state interaction, but rather the *shape* of this peak, especially its width. This is demonstrated in Fig. 3 where the curve labeled J_{13} represents the laboratory yield which one would expect if the DOS function for the (1, 3) pair were constant for all E_r.

(4) *Other effects.* The possibility of interference between any of the above processes has been considered in Ref. 7. One can, in general, avoid those kinematic regions where such interferences can take place and this has been done in the present experiment. Rescattering

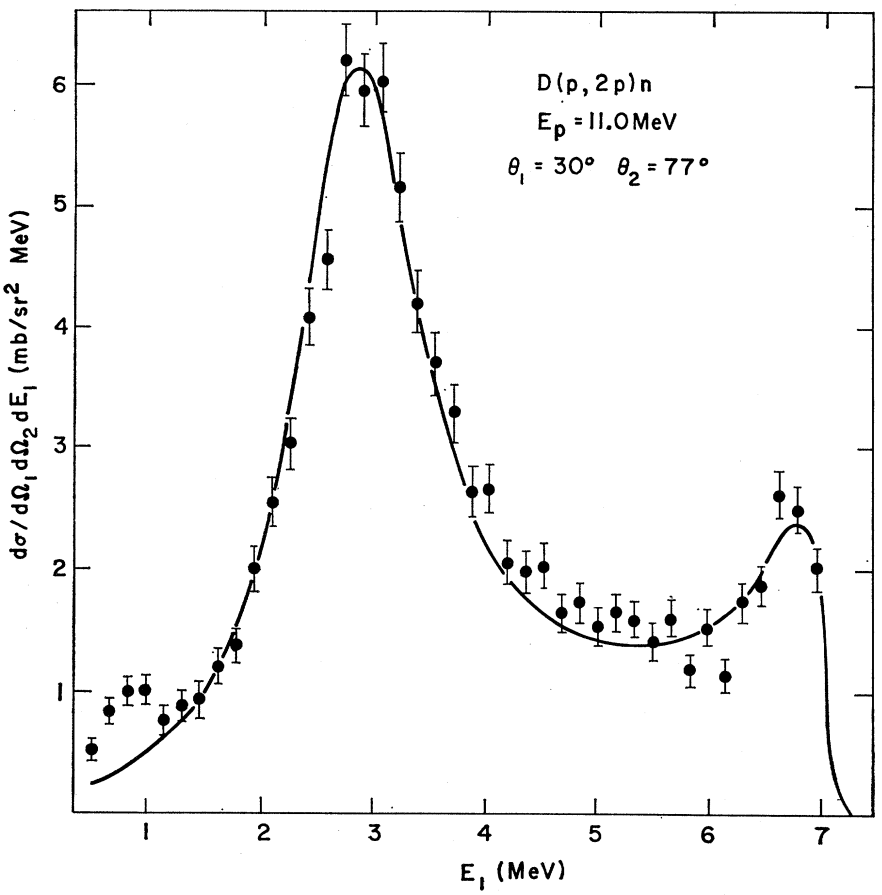

FIG. 4. Fit to the 11-MeV data. The curve gives the fit of the data obtained with a linear sum of the three terms $A\rho_{13}{}^sJ_{13}+B\rho_{12}{}^sJ_{12}+C\rho_{23}{}^sJ_{23}$. The addition of a fourth term HJ_{13} results in a slightly poorer $\chi_n{}^2$ for the fit but only the highest channels of the 3-MeV peak show a small difference. The peak at $E_1<11$ MeV is due to $^{12}C(p, p)$ elastic scattering and is not, of course, fit by the density-of-states formalism. The calculated curve has folded into it kinematic broadening due to finite solid angles, the detector energy resolution function, and energy losses in the target.

as discussed by Valković *et al.*[12] and represented by the triangle graph of Fig. 1(e) of Ref. 7 is possible generally when the FSI in the first step is at a high relative energy. In the p+D breakup reaction, the proton and neutron interacting in the d^* do not have enough separation energy to allow either nucleon to catch up to the first emitted proton. Thus, rescattering has been ignored in subsequent analysis.

The total yield in the $D(p, 2p)n$ reaction, when projected on the E_1 axis, can be expressed as

$$Y_{\rm tot}=A\rho_{13}{}^sJ_{13}+B\rho_{12}{}^sJ_{12}+C\rho_{23}{}^sJ_{23}+D\rho_{13}{}^sJ_{13}+E\rho_{23}{}^tJ_{23}+Fm_{qf}+GP+HJ_{13}, \quad (4)$$

where the ρ's are the appropriate PGB density-of-states functions (Fig. 2), m_{qf} is the square of the quasifree amplitude, the J's are the particle-pair c.m.-to-laboratory solid-angle transformations and P is the phase-space factor. The transformation Jacobians are given by

$$J_{ij}=[(m_1+m_2+m_3)/m_1m_2m_3](1/p_kp_i{}^{(k)})P(E_1, \Omega_1, \Omega_2),$$

where p_k is the momentum of particle k in the c.m. of the $k+(ij)$ system, $p_i{}^{(k)}$ is the momentum of particle i in the (ij) c.m. system, and $P(E_1, \Omega_1, \Omega_2)$ is the phase-space factor. The interaction leading to the first step of the sequential decay process [see Eq. (1)] is assumed momentum independent and is thus included in with the constants A through H.

The effort to isolate the (1, 3) singlet effect from all the others rests on the fact that its structure is significantly different from all the other processes. Observation of Fig. 3 shows that terms 3, 4, 5, and 7 of Eq. (4) have essentially the same structure in the region of the main $\rho_{13}{}^sJ_{13}$ peak and can thus be lumped into a single term whose shape is given by $\rho_{23}{}^sJ_{23}$. The quasifree term is ignored according to earlier arguments. A minimum χ^2 fit to the 11-MeV, $\theta_1=30°$, and $\theta_2=77°$ data was thus made with the four-term expression

$$Y_{\rm tot}=A\rho_{13}{}^sJ_{13}+B\rho_{12}{}^sJ_{12}+C\rho_{23}{}^sJ_{23}+HJ_{13} \quad (5)$$

with

$$\chi_n{}^2=(K-N)^{-1}\sum_{i=1}^{K}\left(\frac{Y_{\rm tot}(i)-Y_{\rm expt}(i)}{[Y_{\rm expt}(i)]^{1/2}}\right)^2. \quad (6)$$

The number of points in the spectrum is denoted by K, N is the number of degrees of freedom, and $Y_{\rm expt}(i)$ is the experimental yield in the ith channel. With the four-term expression of Eq. (4) for $Y_{\rm tot}$, a $\chi_n{}^2$ of 1.87 was obtained. However, the coefficient H had a small

[12] V. Valković, C. Joseph, A. Niiler, and G. C. Phillips, Nucl. Phys. **A116**, 497 (1968).

negative value with the uncertainty overlapping zero. Furthermore, in the highest channels of the principal peak, the only region where the fourth term can be large, its contribution amounted to less than 1% of the contribution from the first term. Consequently, the last term was removed and doing the fit with the first three terms, namely,

$$Y_{\text{tot}}=A\rho_{13}{}^{s}J_{13}+B\rho_{12}{}^{s}J_{12}+C\rho_{23}{}^{s}J_{23}, \tag{7}$$

a $\chi_n{}^2$ of 1.85 was obtained.

Figure 4 shows the fit to the data obtained with the three-term expression. The four-term expression superimposes this curve except for a very slight difference at the top of the main peak. The conclusion, thus, is that no shape due to the HJ_{13} is present in the data and that the spectrum is quite well fit with the three-term expression of Eq. (7). Hence, the yield due to the (1, 3) singlet final-state interaction is

$$Y_{13}=A\rho_{13}{}^{s}J_{13}=Y_{\text{expt}}-B\rho_{12}{}^{s}J_{12}-C\rho_{23}{}^{s}J_{23}. \tag{8}$$

At this point the expression for Y_{13} is a stepwise function. Because further analysis is considerably simplified by using an analytic expression for Y_{13}, a twentieth-order orthogonal polynomial fit of the second half of Eq. (8) was made. The coordinate system traveling with the c.m. of the recoiling d^* is henceforth called the RCM system.

Now, in the two-step sequential decay process $(p+\text{D}\rightarrow p+d^*\rightarrow p+p+n)$, the d^* breaks up into a cone in the laboratory such that a number of the breakup protons will miss the detector. The solid angle into which these breakup protons are deposited is wholly a function of the reaction kinematics, i.e., the total energy, the emission angles of the proton and d^*, and the internal energy E_r of the d^*. The fraction of breakup protons detected is, thus, a function of $\theta_{1/2}$, the direction of the d^* recoil, and the angular distribution of the breakup protons in the RCM system. By calculating the ratio of the number of breakup protons detected to the number of d^*'s produced, one can then determine the differential cross section for the (p, d^*) reaction on deuterium. This calculation is basically a solid-angle transformation.

The input data consist of Y_{13} of Eq. (8) which is the yield of $\text{D}(p, 2p)n$ events due to a reaction in which the first emitted proton scatters at angle θ_2 and a d^* recoils at angle θ_1 before it breaks up into a proton and neutron. The threshold on the energy of the first emitted proton (E_2) is such that only events from the upper part of the locus in the E_1-E_2 plane (see Fig. 1) are accepted. This threshold condition is necessary to make the E_{13} relative energy a single valued function of E_1. However, E_1 is a double-valued function of E_{13}. From now on E_{13} is referred to simply as E_r.

Of the total number of d^*'s produced, the fraction detected (Y^f) is the same in the laboratory as in the RCM systems. Since there are two values of E_1 $(E_1\pm)$ for each value of E_r, the fractional yield in the RCM system as a function of E_r is

$$Y_{\text{RCM}}{}^{f}(E_r)=Y_L{}^{f}(E_1{}^{+})+Y_L{}^{f}(E_1{}^{-}), \tag{9}$$

and the fraction of d^*'s of energy E_r that are detected is

$$\begin{aligned}F_{d^*}&=Y_{\text{RCM}}{}^{f}(E_r)/N_T(E_r)\\&=[Y_L{}^{f}(E_1{}^{+})+Y_L{}^{f}(E_1{}^{-})]/N_T(E_r),\end{aligned} \tag{10}$$

being the same in both the lab and RCM systems. $N_T(E_r)$ is the total number of d^*'s of energy E_r that are produced. The fraction of the total RCM solid angle seen by detector 1 is

$$F_\Omega=[d\Omega_{\text{RCM}}(E_r, E_1{}^{+})+d\Omega_{\text{RCM}}(E_r, E_1{}^{-})]/4\pi, \tag{11}$$

where the $d\Omega_{\text{RCM}}$'s are the detector-1 solid angles transformed into the RCM system and are given by

$$d\Omega_{\text{RCM}}(E_r, E_1)=d\Omega_1/G(E_r, E_1), \tag{12}$$

where

$$G(E_r, E_1)=[1/2(E_f+E_r)][E_r{}^2-E_fE_r\sin^2(\psi-\zeta)]^{1/2}.$$

Here

$$E_f=(4/9)[E_1+3Q+(E_1{}^2+\tfrac{3}{2}QE_1)^{1/2}]\cos\alpha,$$

ψ is the lab angle of the first emitted proton, ζ is the lab angle of the d^*, α is the c.m. angle of the d^*, and the proton and neutron masses are taken as 1 and the deuteron mass as 2.

Now the d^*, being in a $^1S_0$ configuration, breaks up isotropically in the RCM system. Thus, the fraction of the breakup protons detected is equal to the fraction of the RCM solid angle observed. Combining Eqs. (10) and (11), the total number of d^*'s produced is

$$N_T(E_r)=4\pi\,\frac{Y_L{}^{f}(E_1{}^{+})+Y_L{}^{f}(E_1{}^{-})}{d\Omega_{\text{RCM}}(E_r, E_1{}^{+})+d\Omega_{\text{RCM}}(E_r, E_1{}^{-})}, \tag{13}$$

and the cross section for the p, d^* reaction as a function of E_r becomes

$$d^2\sigma/dE_rd\Omega=N_T(E_r)/N_bN_t\Delta\Omega_L{}', \tag{14}$$

where N_b and N_t are the number of bombarding and target particles, respectively, and $\Delta\Omega_L{}'$ is the laboratory solid angle into which the d^*'s are allowed. $\Delta\Omega_L{}'$ is given by the $p+\text{D}\rightarrow p+d^*$ reaction solid-angle transformation

$$d\Omega_L{}'=Jd\Omega_2, \tag{15}$$

where $d\Omega_2$ is the laboratory solid angle of detector 2 which detects the first emitted proton.

$$J=(\sin^2\zeta/\sin^2\psi)[\cos(\alpha-\zeta)/\cos(\beta-\psi)],$$

where ζ, ψ, and α are defined above, and β is the c.m. angle of the first emitted proton. The N_bN_t product is obtained from a simultaneous $p+\text{D}$ elastic scattering experiment where the recoil deuteron is observed in detector 1:

$$N_bN_t=N_{\text{el}}/\sigma_{\text{el}}\Delta\Omega_1, \tag{16}$$

where N_{el} is the number of recoil deuterons counted, σ_{el}

is the elastic cross section, and $\Delta\Omega_1$ is the detector-1 solid angle.

Since the calculation if done in terms of E_r but the Y^l's are functions of E_1, the Y^l's must be corrected by a factor $(1/\Delta E_1)(\partial E_1/\partial E_r)$, where E_1 is the energy width of the data channels.

Finally, substituting all appropriate quantities into Eq. (14), the cross section for the production of d^* as a function of E_r becomes

$$d^2\sigma/dE_r d\Omega = (4\pi\sigma_{el}/JN_{el}\Delta E_1\Delta\Omega_2) \times \frac{Y_L{}^l(E_1{}^+)(\partial E_1{}^+/\partial E_r)+Y_L{}^l(E_1{}^-)(\partial E_1{}^-/\partial E_r)}{1/G(E_r, E_1{}^+)+1/G(E_r, E_1{}^-)} . \quad (17)$$

The results of Eq. (17) are plotted in Fig. 5 for the bombarding energies 9.0, 10.0, 11.0, and 12.0 MeV. These are typical results, all other energies showing similar structure. In each case $d^2\sigma/dE_r d\Omega$ has a maximum slightly below 100 keV and then falls smoothly until E_r equals 0.4–0.5 MeV. Beyond that value, there are spurious wiggles which are attributable to the fact that the data in these regions were statistically poor. Typical uncertainties, due to statistics, are shown for $E_r=0.35$ MeV.

RESULTS AND DISCUSSION

A. D(p, d^*)p Cross Section

The results of the calculation in the previous section pictured in Fig. 5 show that for a given total system

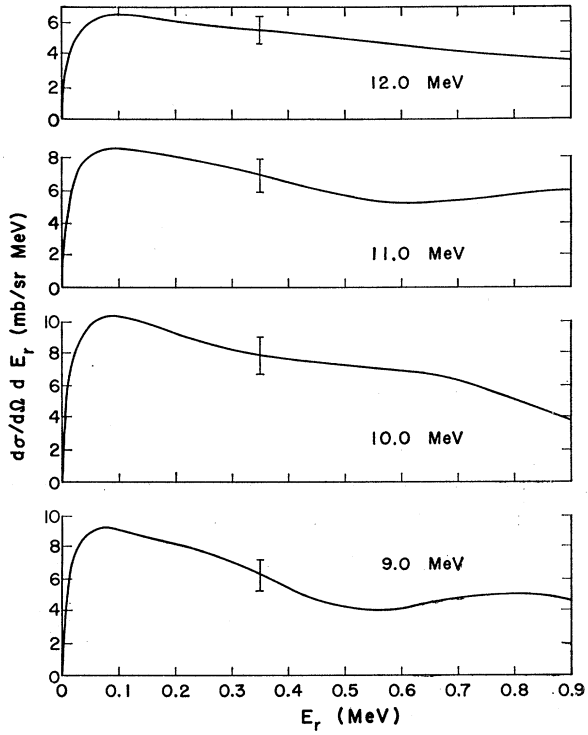

FIG. 5. $d\sigma/dE_r d\Omega(E_r)$ for four energies, 9.0, 10.0, 11.0, and 12.0 MeV. A sample of the experimental uncertainty due to statistics is shown for each curve at $E_r=0.35$ MeV.

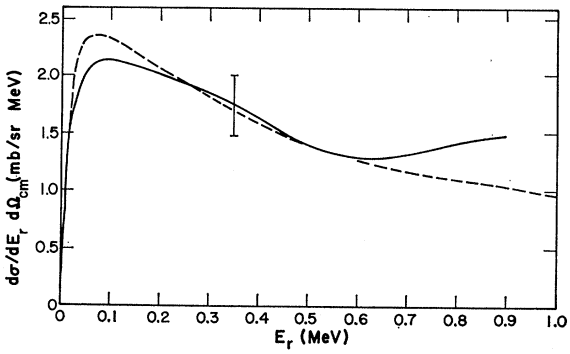

FIG. 6. Comparison of the $d\sigma/dE_r d\Omega_{c.m.}(E_r)$ at 11 MeV with the predicted shape of the d^* structure from the ^{9}Be$(p, d^*)^8$Be reaction (Ref. 12).

energy, the cross section for the production of the n-p quasiparticle varies as a function of E_r. This structure, in general, rises sharply from zero to a maximum near $E_r=80$ keV and then, within experimental uncertainty, drops monotonically to about half the maximum value near $E_r=1$ MeV.

In a calculation of the ^{9}Be$(p, d^*)^8$Be cross section, Kolltveit and Nagatani[13] have obtained the structure of the $d\sigma/d\Omega_{c.m.}dE_r(p, d^*)$ as a function of E_r. They calculated both the (p, d^*) and (p, d) cross sections with the distorted-wave Born approximation (DWBA), using a zero-range two-nucleon potential whose strength is determined from the effective range theory. The p-n final state was treated as a free scattering state. The structure of the d^* should, of course, be independent of the reaction through which it is formed. Thus, one can compare their calculated results with the present experimental result. Figure 6 shows our experimental curve now transformed into the p-d^* c.m. system (solid line) along with Kolltveit and Nagatani's curve (dashed). The calculated curve is normalized to the experimental curve. It can be seen that, within experimental uncertainty, the two curves agree quite well.

It should be noted that the experimental shape is in agreement with assertions that the d^* is a short-lived composite of a neutron and proton. The peak at low E_r is an indication that the neutron and proton leave the vicinity of the first emitted proton before breaking up. Also of interest is the fact that $d\sigma/dE_r d\Omega$ goes to zero at $E_r=0$, while the density-of-states function given by the energy derivative of the phase shift starts at a high value at $E_r=0$ and decreases monotonically with increasing E_r.

Now the (p, d^*) cross section can be written as

$$\frac{d\sigma}{d\Omega}(p, d^*) = \int_0^{E_r(\max)} \frac{d\sigma}{dE_r d\Omega} dE_r, \quad (18)$$

where $E_r(\max)$ is the maximum E_r for which we consider the n-p system to constitute the d^* particle. A

[13] K. Kolltveit and K. Nagatani, Nucl. Phys. **A124**, 287 (1969).

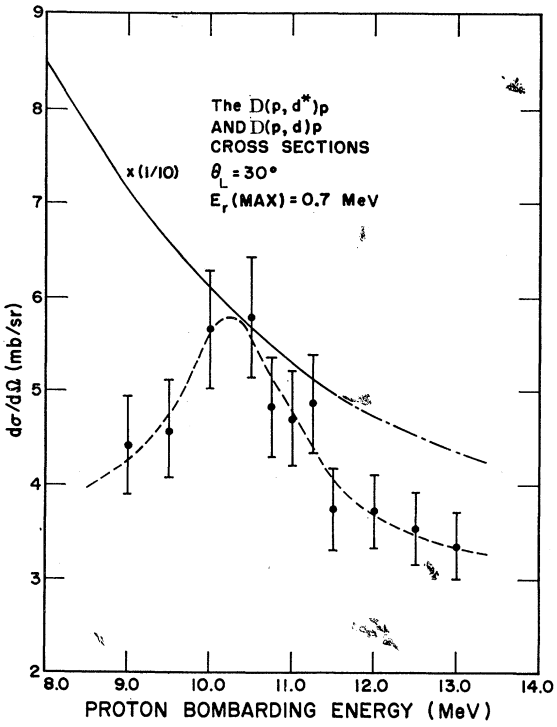

FIG. 7. $d\sigma/d\Omega(p, d^*)$ and $d\sigma/d\Omega(p, d)$ at $\theta_L=30°$ plotted as a function of the proton bombarding energy. The (p, d^*) cross sections, derived from Eq. (18), are the result of integrating Eq. (17) to $E_r(\max)-0.7$ MeV. The error bars represent absolute uncertainties in the cross sections.

priori, the appropriate value for $E_r(\max)$ would be that value of E_r at which $d\sigma/dE_r d\Omega(E_r)$ drops to half of its maximum value. According to Kolltveit and Nagatani's calculation, this value should be $E_r=0.7$ MeV. However, in order to determine the effect of $E_r(\max)$ on the shape of the $D(p, d^*)p$ excitation function, the cross section [Eq. (18)] was integrated to four values of $E_r(\max)$, 0.3, 0.5, 0.7, and 0.9 MeV. The result of the integration to 0.7 MeV is shown in Fig. 7. In this figure, the $D(p, d)p$ elastic cross section ($\times\frac{1}{10}$) is also shown for comparison. The dot-dashed part of that curve is an extrapolation of the solid curve beyond the bombarding energy where the data for the elastic cross section stopped. The dashed curve is a free-hand fit of the (p, d^*) excitation function. The ratio $R=\sigma(p, d)/\sigma(p, d^*)$ can be expected to lie between 5 and 20 for various reactions[8,13] and should decrease with increasing energy. This ratio is near 10 for the proton on deuterium processes. However, by observing Fig. 8 where the results of the integration of Eq. (18) are shown to four values of $E_r(\max)$, one can see that the ratio R is a strong function of $E_r(\max)$. The error bars in Figs. 7 and 8 denote absolute errors, of which all but 3.5% are due to relative uncertainty.

A smooth curve drawn under the peak such that it follows the general downward trend of the cross section would represent the nonresonant part of the cross section. The ratio of peak value to nonresonant part of the $d\sigma/d\Omega$ at the energy of the peak remains constant within statistical uncertainties for all four ranges of integration. Thus, the peaking effect remains essentially the same although from Fig. 8 it seems that there is an increase with $E_r(\max)$.

A summary of the $d\sigma/d\Omega(p, d^*)$ results is given in Table II.

B. Excited States of ^{3}He

A renewed effort has gone into the search for excited states of ^{3}He since the report by Kim *et al.*[14] of three

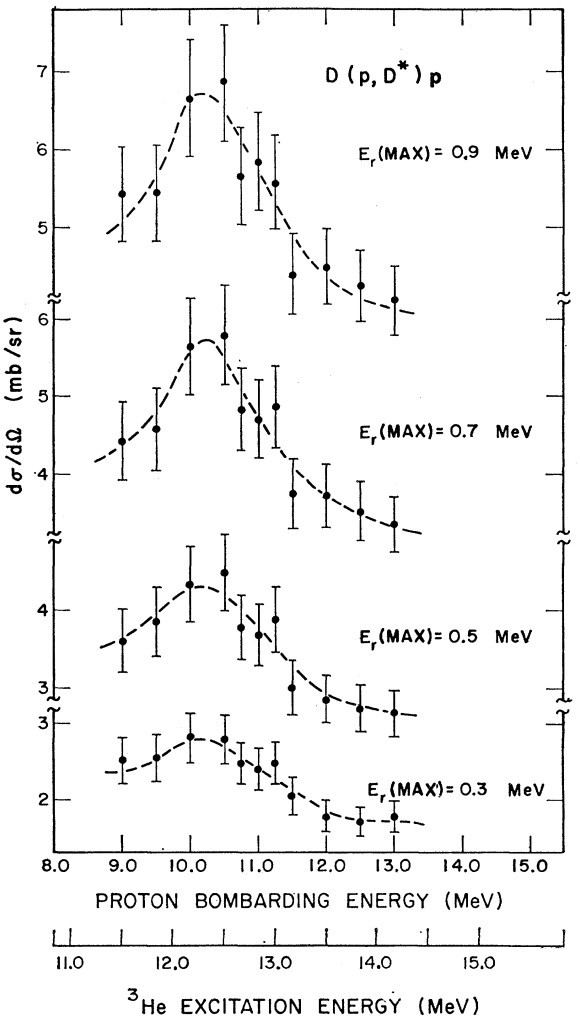

FIG. 8. $d\sigma/d\Omega(p, d^*)$ as a function of $E_r(\max)$. The (p, d^*) excitation function is shown for the four values of $E_r(\max)$: 0.3, 0.5, 0.7, and 0.9 MeV. The error bars represent absolute uncertainties. A peak at $E_p=10.25$ MeV is seen in all cases with the same relative intensity. This peak occurs at a ^{3}He excitation energy of 12.4 MeV.

[14] C. C. Kim, S. M. Bunch, D. W. Devins, and H. H. Forster, Phys. Letters **22**, 314 (1966).

TABLE II. Summary of experimental cross sections.[a]

E_p	$d\sigma/d\Omega(p, d^*)$ 0.3 MeV	$d\sigma/d\Omega(p, d^*)$ 0.5 MeV	$d\sigma/d\Omega(p, d^*)$ 0.7 MeV	$d\sigma/d\Omega(p, d^*)$ 0.9 MeV	$d\sigma/d\Omega(p, d)$	R[b]
9.00	2.49±0.39	3.59±0.41	4.42±0.50	5.42±0.61	71.0±3.0%	16.18
9.50	2.52±0.29	3.84±0.44	4.58±0.52	5.44±0.62	65.8±3.0%	14.37
10.00	2.78±0.31	4.32±0.48	5.65±0.62	6.65±0.74	60.6±3.0%	10.74
10.50	2.75±0.30	4.46±0.49	5.78±0.64	6.86±0.75	56.5±3.0%	9.78
10.75	2.44±0.27	3.76±0.41	4.82±0.53	5.65±0.61	54.4±3.0%	11.27
11.00	2.37±0.26	3.67±0.37	4.70±0.50	5.85±0.62	53.0±3.0%	11.27
11.25	2.48±0.27	3.86±0.42	4.86±0.53	5.58±0.61	50.9±3.0%	10.48
11.50	2.03±0.24	2.98±0.35	3.74±0.44	4.40±0.52	49.5±3.0%	13.24
12.00	1.77±0.19	2.83±0.30	3.72±0.40	4.49±0.48	(45.7)	(12.28)
12.50	1.70±0.19	2.72±0.29	3.52±0.38	4.24±0.46	(42.6)	(12.09)
13.00	1.76±0.19	2.66±0.29	3.35±0.36	4.07±0.43	(40.2)	(11.99)

[a] All cross sections in mb/sr.

[b] $R = [d\sigma/d\Omega(p, d)]/[d\sigma/d\Omega(p, d^*)0.7 \text{ MeV}]$.

narrow states in ^{3}He at 8.2, 10.2, and 12.6 MeV on the basis of the ^{3}He$(p, p')^3$He* reaction. However, subsequent experiments on the same and other reactions have not found any definitive evidence for these states. A summary of these experiments is given in Table III.

TABLE III. Searches for ^{3}He excited states.

Reaction	Results
^{3}He$(p, p')^3$He*	States at $E_x(^3\text{He})$ of 8.2, 10.2, 12.6 MeV[a]
^{3}He$(p, p')^3$He*	No states to $E_x(^3\text{He}) \leq 15$ MeV[b]
^{3}He$(^3\text{He}, ^3\text{He}')^3$He*	Upper limit of 120 μb/sr to $E_x(^3\text{He}) = 30$ MeV[c]
^{6}Li$(p, p\text{-}d)\alpha$	No $T=\frac{1}{2}$ states below $E_x(^3\text{He}) = 11$ MeV[d]
^{6}Li$(p, p\text{-}\alpha)d$	
^{6}Li$(p, d\text{-}\alpha)p$	
^{3}He$(\alpha, \alpha')^3$He*	Upper limit of 300 μb/sr for state at $E_x(^3\text{He}) = 10.2$ MeV[e]
^{6}Li$(p, \alpha)^3$He*	$T=\frac{1}{2}$ states at $E_x(^3\text{He})$ of 10.2 and 12.6 MeV[f]
^{6}Li$(p, \alpha)^3$He*	Some anomalies near $E_x(^3\text{He})$ of 11–12 MeV[g]
D$(p, p)d$	No structure to $E_x(^3\text{He}) = 13.5$ MeV[h]

[a] See Ref. 14.

[b] M. D. Mancusi, C. M. Jones, and J. B. Ball, Phys. Rev. Letters **19**, 1449 (1967); S. A. Harbison, F. G. Kingston, A. R. Johnston, and E. A. McClatchie, Nucl. Phys. **A108**, 478 (1968).

[c] R. J. Slobodrian, J. S. C. McKee, D. J. Clark, W. F. Tivol, and T. A. Tombrello, Nucl. Phys. **A101**, 109 (1967).

[d] V. Valković, C. Joseph, S. T. Emerson, and G. C. Phillips, Nucl. Phys. **A106**, 138 (1967).

[e] R. E. Warner, J. S. Vincent, and E. T. Boschitz, Phys. Letters **24B**, 91 (1967).

[f] H. H. Forster, J. Hokhikiou, and C. C. Kim, International Conference on Nuclear Physics, Gatlinburg, 1966 (unpublished).

[g] D. K. Olsen and R. E. Brown, Phys. Rev. **176**, 1192 (1968).

[h] See Ref. 11.

A number of partial-wave analyses of the nucleon-deuteron scattering[15–17] have given good fits to angular distributions up to 30 MeV. Although some of the phase shifts have very slow positive excursions near the ^{3}He excitation energies of 7 and 12 MeV, the interpretation of these excursions as states of ^{3}He is questionable.

In Fig. 8, the excitation function of the D$(p, d^*)p$ reaction is shown for four values of E_r(max) and, in all cases, a bump persists at a bombarding energy of about 10.25 MeV. The corresponding energy of excitation in ^{3}He is shown in the bottom scale indicating that the observed structure is at a ^{3}He excitation energy of 12.4 MeV. Since the experimental constraints require that the reaction proceed via the $p+d^*$ channel, it is quite likely that the observed peak has a $(p\text{-}d^*)$ cluster structure.

If this structure were due to a resonance in ^{3}He, one might expect to see such a resonance in the $d(p, d)p$ elastic channel also since a $T=\frac{1}{2}$ component must be present due to the incident channel isospin. However, the elastic scattering excitation function shows no structure which can be associated with a state in ^{3}He near 12.5 MeV. Assuming that the $(p\text{-}d^*)$ cluster structure is a good description of this state, then to see it in the elastic (p, d) channel, the deuteron spin must be flipped twice, whereas only one flip is necessary to see it in the (p, d^*) channel. One expects that the spin-flip amplitude is much less than the no-spin-flip amplitude; thus, the cross section for observing this $(p\text{-}d^*)$ state via the elastic channel would be much smaller than in the inelastic channel. For example, if the ratio of the spin-flipped to non-spin-flipped amplitude is as large as 10^{-1}, one should see only ~0.2-mb cross section in the elastic channel. The uncertainties on the elastic scattering excitation function by Wilson[11] are about ±2.5 mb.

[15] W. T. H. van Oers and K. W. Brockman, Jr., Nucl. Phys. **A92**, 561 (1967).

[16] R. Aaron, R. D. Amado, and Y. Y. Yam, Phys. Rev. **140**, B1291 (1965).

[17] J. Arvieux, Nucl. Phys. **A102**, 513 (1967).

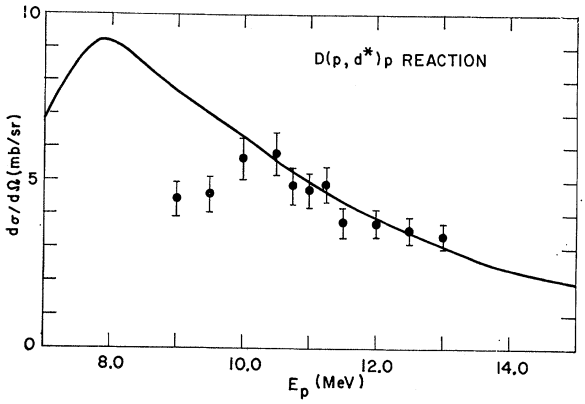

FIG. 9. D(p, d^*)p cross section at $\theta_{d^*}=30°$ in the lab. The solid curve shows the results of the Frank-Gammel zero-range calculation. The dots represent the present data. E_r(max) = 0.7 MeV for both calculation and data. There is no relative normalization between calculated curve and data.

Thus, even though the state has a pure $T=\frac{1}{2}$ isospin, it would not be observable in (p-d) elastic-scattering experiments with present accuracies. The probability of seeing a predominantly $T=\frac{3}{2}$ state of ^{3}He in the elastic channel is even smaller since in this case double isospin violation is added to the small spin-flip amplitudes. An elastic p-d scattering experiment with much better precision than those done to date may show evidence for a $T=\frac{1}{2}$ state while it is highly unlikely that such an experiment could show a predominantly $T=\frac{3}{2}$ state. Although no $T=\frac{1}{2}$ or $\frac{3}{2}$ states in ^{3}He have been definitely identified through the ^{3}He(p, p') and ^{3}He(^{3}He, ^{3}He′) reactions, a (p-d^*) cluster state might have a very low probability of being excited by these reactions.

C. Threshold Effect

The zero-range theory of Frank and Gammel[18] was used to calculate the triple differential cross section for the D(p, $2p$)n reaction from E_p=7–15 MeV and the proton angles corresponding to the (p, d^*) recoil axis. Over the energy range where the calculation overlaps the experiment, there is generally good agreement except for the lowest energy experimental points of 9 and 9.5 MeV. There, the calculated cross sections are higher than the experimental.

[18] R. M. Frank and J. L. Gammel, Phys. Rev. **93**, 463 (1954).

The calculated cross sections were analyzed the same way as the experimental data resulting in the (p, d^*) cross sections. [See Eq. (8) and following in Analysis section.] The theoretical excitation function for the $d\sigma/d\Omega(p, d^*)$ shows a rise from 7 to 8 MeV and then a monotonic fall to 15 MeV. From 10 MeV on, the theoretical cross section agreed very well with the experimental. The main disagreements between experimental and theoretical excitation functions are the position of the maxima (8 MeV for theoretical and 10.25 for experimental) and that the cross section at the maximum is higher in the theoretical curve than in the experimental. This theoretical curve and the experimental points are shown in Fig. 9.

The Frank-Gammel theory includes no factors which could produce a resonance in the three-body system. Rather, the cross section is given by the product of a phase-space term which increases with energy and the square of a matrix element which decreases with energy. Thus, the shape of the theoretical excitation function can be explained by a rise in the cross section due to increasing phase space from the 3.33-MeV threshold to a point where the decreasing matrix element squared becomes dominant. This is the usual threshold effect. Because of the approximations in the zero-range theory of Frank and Gammel, it is not surprising that the experimental and theroretical maxima are about 2 MeV apart. A more exact calculation, possibly with separable potentials, should give a better agreement with the experiment.

In conclusion, it should be stated that an experiment with considerably better statistics, especially in regions where E_r approaches 1 MeV, is necessary. Although the Frank-Gammel calculation indicates that the peaking effect in the D(p, d^*)p excitation function is possibly due to threshold effect, until more exact calculations are done, a broad state in ^{3}He at 12.4 MeV composed of a (p-d^*) cluster that is excited in the D(p, d^*)p reaction cannot be ruled out.

ACKNOWLEDGMENTS

One of us (A.N.) wishes to express his appreciation to Dr. J. C. Hopkins and Dr. P. W. Keaton for valuable discussions during the preparation of this paper and to Dr. D. Dodder and Dr. J. L. Gammel for the unpublished results of the zero-range calculation.